Alternative approaches to infrared multiphoton dissociation in an external ion reservoir

ARTICLE *in* JOURNAL OF THE AMERICAN SOCIETY FOR MASS SPECTROMETRY · JANUARY 2004

Impact Factor: 2.95 · DOI: 10.1016/j.jasms.2003.08.007 · Source: PubMed

Alternative Approaches to Infrared Multiphoton Dissociation in an External Ion Reservoir

Steven A. Hofstadler, Jared J. Drader, Hans Gaus, James C. Hannis, and Kristin A. Sannes-Lowery
Ibis Therapeutics, a Division of Isis Pharmaceuticals, Carlsbad, California, USA

In this work we present variations on in-hexapole infrared multiphoton dissociation (IRMPD) for the characterization of modified oligonucleotides using an ESI-FTICR spectrometer. We demonstrate that IRMPD in the external ion reservoir provides a comprehensive series of fragments allowing thorough characterization of a wide range of oligonucleotides containing alternative backbones and 2′ substitutions. An alternative pulse sequence is presented that allows alternating MS and IRMPD MS/MS spectra to be acquired on a chromatographic timescale without loss in ionization duty cycle. Ions are excited to a larger cyclotron radius such that they "dodge" the IR laser beam that travels through the center of the trapped ion cell and impinges on the external ion reservoir creating IRMPD fragments that will be detected in the next scan. An alternative approach for directing IR radiation into the external ion reservoir using a hollow fiber waveguide as a photon conduit is presented. This approach offers a simple and robust alternative to the previously utilized on-axis scheme and may allow effective implementation with lower power lasers owing to the inherent increase in power density achieved by focusing the nascent laser beam into the hollow fiber waveguide. (J Am Soc Mass Spectrom 2003, 14, 1413–1423) © 2003 American Society for Mass Spectrometry

Infrared multiphoton dissociation (IRMPD) has previously been shown to be an effective means for dissociating macromolecular ions providing sequence and/or structure information in conjunction with mass spectrometric detection. Following the earlier work of Beauchamp and coworkers [1] and Eyler and coworkers [2], McLafferty and coworkers demonstrated the applicability of IRMPD for the efficient fragmentation of proteins [3] and oligonucleotides [4] in the trapped ion cell of an FTICR. While perhaps somewhat slow to gain broad acceptance, IRMPD is beginning to see broader usage [3–7] and is now commercially available on FTICR instruments.

Marshall and coworkers have previously demonstrated that prior to mass analysis by FTICR, ions generated by electrospray can be accumulated in an external ion reservoir comprised of an rf-only multipole bounded by electrostatic elements [8]. This approach not only improves the ionization duty cycle to near unit efficiency, but affords the opportunity to manipulate the ion ensemble prior to mass analysis. We recently demonstrated that infrared multiphoton dissociation can be performed in this external ion reservoir by passing an unfocused laser beam through the ion volume during, or following, the external ion accumulation event [9]. In addition to providing a simple, platform-independent IRMPD scheme, this method generates improved fragment ion abundance and sequence coverage for oligonucleotide ions relative to in-cell IRMPD at low pressure ($<10^{-9}$ torr). This enhanced sequence coverage is likely due to the stabilizing effect of multiple low energy collisions in the hexapole that collisionally cool primary metastable fragment ions that would otherwise follow additional dissociation pathways. Thus, collisionally cooling these vibrationally activated ions below their dissociation threshold results in larger, more highly charged primary fragment ions. In this work we expand upon the previously presented in-hexapole IRMPD studies and demonstrate new applications of the approach including a scheme for alternating between MS and MS/MS measurements during an LC separation, and a new approach for bringing IR radiation into the external ion reservoir using a hollow fiber waveguide as a photon conduit.

Experimental

Mass Spectrometry

All experiments were performed on a Bruker Daltonics (Billerica, MA) Apex 70e Fourier transform ion cyclo-

Published online October 23, 2003

Address reprint requests to Dr. S. A. Hofstadler, Ibis Therapeutics, a Division of Isis Pharmaceuticals, Inc., 2292 Faraday Avenue, Carlsbad, CA 92008, USA. E-mail: shofsatd@isisph.com

1044-0305/03/$30.00
doi:10.1016/j.jasms.2003.08.007

Received July 7, 2003
Revised August 19, 2003
Accepted August 19, 2003

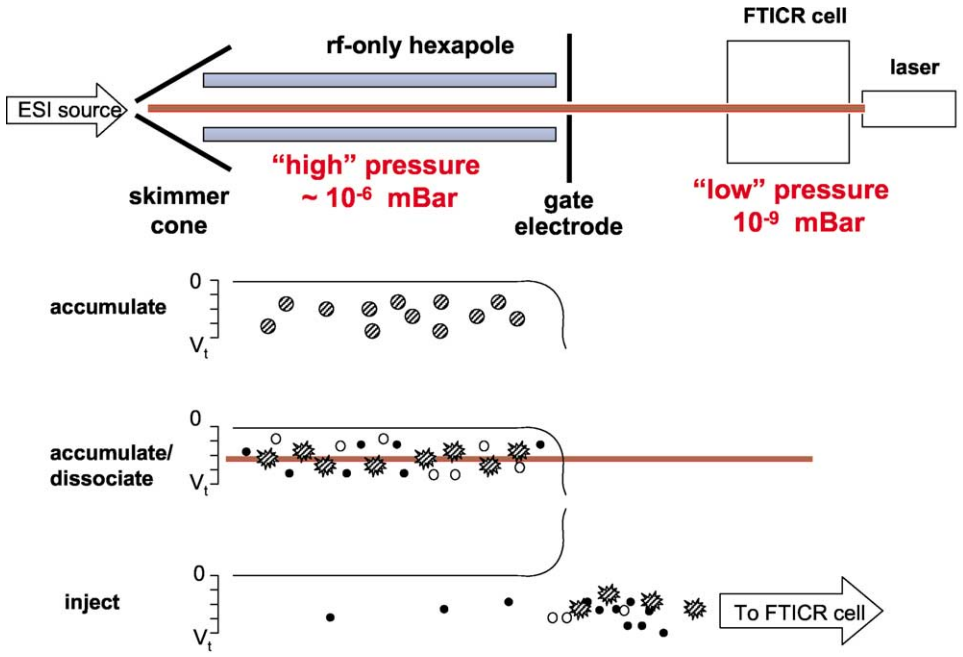

Figure 1. Experimental configuration for performing on-axis IRMPD in an external ion reservoir. The unfocused beam of a 25 W CO_2 laser is aligned to be coaxial with the central axis of the rf-only hexapole. Ions are accumulated and dissociated in the high pressure (5×10^{-6} mbar) external ion reservoir prior to being transferred to the FTICR trapped ion cell where they are mass analyzed.

tron resonance mass spectrometer. The spectrometer is equipped with an Analytica (Branford, CT) electrospray source utilizing a grounded ESI emitter, a glass desolvation capillary with countercurrent drying gas, and an external ion reservoir. The external ion reservoir consists of a biased skimmer cone, an rf-only hexapole ion guide and a gate electrode at the low-pressure end of the hexapole ion guide. Ions are accumulated in the external ion reservoir (concurrent with and/or preceding IR irradiation for the IRMPD experiments) for 0.5–1 s and pulsed into the modified Infinity trapped ion cell for analysis by FTICR [6]. The oligonucleotides were analyzed in the negative mode with the potential applied to the capillary exit maintained at −50 V to avoid nozzle-skimmer fragmentation. The skimmer cone voltage is held at 0 V and the gate electrode toggles between −20 V during accumulation and 20 V during ion ejection. The ions are excited and detected over an *m/z* range of 440–5000. Thus, fragment ions with *m/z* values <440 such as a_2-B and w_1 are not observed under these experimental conditions. All aspects of the experiment including data acquisition, processing, and plotting were performed using Bruker XMASS version 5.0 software running on a dual processor Pentium PC.

Model Oligonucleotides

A collection of four model oligonucleotides, synthesized in-house, were used in these studies. ***Oligo1*** is a 20-mer phosphorothioate oligonucleotide (GCCCAAGCTGG CATCCGTCA, MW = 6363.612), ***oligo2*** is 4-10-4 MOE "gapmer" phosphorothioate oligonucleotide (GATGC-CAGAGAGGATGCC, MW = 6490.9459) in which the underlined bases represent a methoxyethyl (MOE) modification at the 2′ sugar position in the "wings" and a normal 2′ deoxy group in the "gap", ***oligo3*** is a 15-mer phosphodiester oligonucleotide (GGGTTCCCTAGT-TAG, MW = 4596.791), and ***oligo4*** is a 24-mer phosphorothioate oligonucleotide (CCAGGCGCCGCGAGCGC-CTCTCAT MW = 7639.707). The phosphorothioate modification, which renders oligonucleotides more refractory to exonuclease digestion, involves the substitution of an oxygen atom of the normal phosphodiester backbone with a sulfur atom.

HPLC

A 1 μL aliquot containing a mixture of 3 oligonucleotides, (***oligo1, oligo3, and oligo4***) at a concentration of 2 μM each was loaded onto 180 μm × 20 cm (fused silica) column packed with Luna C18. With a post splitter flow rate of 1.5 μL/min a linear solvent gradient beginning at 60% solvent A (2 mM tripentylammoniumacetate in 30% acetonitrile) and 40% solvent B (2 mM tripentylammoniumacetate in 90% acetonitrile) evolved to 15% solvent A over a 30 min period.

IRMPD

As shown in Figure 1, the external ion accumulation region is comprised of a biased skimmer cone, an rf-only hexapole operating at 5 MHz (500 $V_{p\text{-}p}$), and an

auxiliary "gate" electrode at the low pressure end of the hexapole. A 25 watt CW CO_2 laser (Synrad Inc., Mukilteo, WA) operating at 10.6 μm was used for all IRMPD experiments. IRMPD of ions in the external ion reservoir was effected by irradiation during the ion accumulation event. For on-axis irradiation, a lab-built aluminum optical bench was positioned approximately 1.5 m from the actively shielded superconducting magnet such that the laser beam was aligned with the central axis of the magnet. Using standard IR-compatible mirrors and kinematic mirror mounts, the unfocused 3.5 mm laser beam was aligned to traverse directly through the 3.5 mm holes in the trapping electrodes of the modified Infinity trapped ion cell and longitudinally traverse the hexapole region of the external ion guide finally impinging on the skimmer cone [6]. Alignment was accomplished by a preliminary visual alignment with a visible diode laser such that light could be seen exiting the glass desolvation capillary at the source-end of the spectrometer. Subsequent alignment was optimized by the mass spectral fragmentation response with the IR laser triggered during the ion accumulation interval. For orthogonal irradiation, a 1 mm i.d. hollow fiber waveguide (Polymicro, Inc, Tucson, AZ) was employed. As described in detail elsewhere [10], the waveguide vacuum interface assembly was mounted within an x,y translator stage housing an aluminum beam-aperture with a 1 mm diameter orifice and a 13 mm diameter by 2 mm thick BaF_2 window (Saint-Gobain Crystals and Detectors, Solon, OH). A vacuum chamber is created between the BaF_2 window and the hollow fiber waveguides (HFWG) by compressing a Viton O-ring against the BaF_2 window and compressing a second Viton O-ring around the exterior of the HFWG. The exit end of the HFWG enters the external ion reservoir orthogonal to the ion axis through another vacuum interface created by compressing a Viton O-ring against the exterior of the HFWG.

Results and Discussion

Sequence Characterization of Modified Oligonucleotides

Antisense compounds are generally short 15–20 mer synthetic oligonucleotides that bind messenger RNA and inhibit the expression of genes associated with metabolic disorders, cancer, and infectious diseases [11]. Modifications to the standard phosphodiester linkages and 2′deoxyribose sugars are generally employed to increase the binding affinity of the oligonucleotides to the messenger RNA and to mitigate in vivo enzymatic degradation [12]. Fast and reliable methods are needed for sequencing such oligonucleotides since standard enzymatic techniques are not compatible with the majority of these modifications.

We recently demonstrated that the in-hexapole IRMPD (InHex IRMPD) approach is a valuable tool for characterizing both uniformly modified and chimeric oligonucleotides (i.e., those with mixed 2′ or backbone modification), including gapmers [13]. We showed that regardless of whether the backbone is comprised of phosphodiester or phosphorothioate linkages, fragmentation of oligodeoxynucleotides generates $a_n - B$ and w_n fragment ions that are most useful for sequence confirmation. Furthermore, coupling this dissociation method with the high performance attributes of FTICR mass spectrometry allows one to extract more information from the resulting complex spectrum than would be afforded by other MS detection platforms. For example, Figure 2 provides an example of the complexity of the spectra that typically result from the InHex dissociation of a 20-mer phosphorothioate oligonucleotide (***oligo1***). The inset in Figure 2a illustrates the cleanly resolved isotope distribution of the $(M - 3H^+)^{3-}$ charge state of the w_7 (McLuckey nomenclature [14]) fragment ion; the average resolution of each isotope peak is in excess of 70,000 (FWHM) and the theoretical and measured masses differ by less than 1.5 ppm. The ability to resolve overlapping isotope distributions allows the extraction of large amounts of information, even when considerable spectral congestion is present. The inset in Figure 2b illustrates that under the spectral acquisition conditions employed, the overlapping a_{10}-base$^{(3-)}$ and a_{13}-base$^{(4-)}$ signals are clearly resolved even though they differ by less than 0.08 *m/z* units and are present at $<$1% of the base peak in the spectrum. The asymmetric shape of the isotope envelope in b) is due to the constructive interference (i.e., non-resolved) associated with the signals from the third and fourth isotope peaks of the a_{10}-base^{3-} and a_{13}-base^{4-} species, respectively. Table 1 shows that rich and redundant sequence coverage is obtained for this 20-mer phosphorothioate oligonucleotide as evidenced by the detection of multiple charge states of multiple fragment ions spanning the entire length of the oligonucleotide. Note that fragmentation on the 3′ side of a T in the TG motif (bases 9 and 10) is not observed in the a-base or w-ion series. As described in detail elsewhere, this is typical of 2′ deoxy oligonucleotides [13]. While the decrease in abundance (or absence) of these fragments may result in sequence gaps in the $a_n - B$ and w_n fragment ions series, c and y ions are typically observed for these motifs allowing one to fill the sequence gaps [13].

Interestingly, modifications to the 2′ position of deoxyribose sugars can have a profound influence on the types and abundances of fragment ions produced. For example, changing the 2′ substituent to a hydroxyl or a methoxyethyl (MOE) group results in dominate b_n/x_n and c_n/y_n fragment ions which still provide useful sequence information. Moreover, in cases where there is a mixture of 2′ substituents (e.g., gapmers), fragmentation occurs predominately at the 2′ deoxy groups. In addition, regardless of the 2′ substituent, fragmentation 3′ to a T is significantly decreased or absent, which may result in gaps in the a_n-B and w_n fragment ions series.

Characteristics of InHex IRMPD fragmentation of

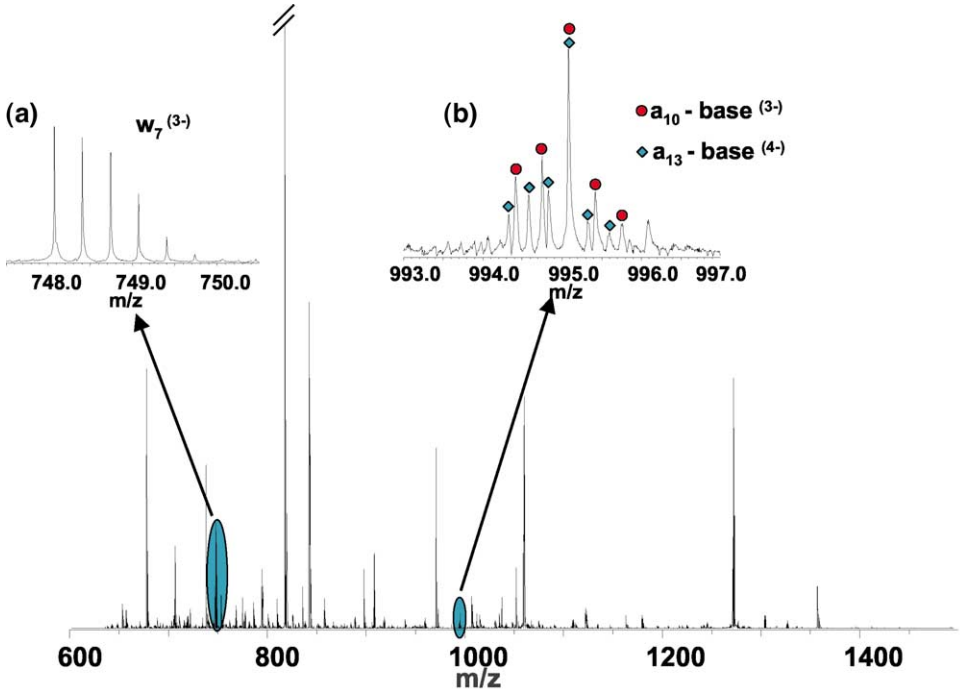

Figure 2. ESI-FTICR mass spectrum produced by in-hexapole IRMPD of a 20-mer phosphorothioate oligonucleotide (***oligo1***). Inset (**a**) shows the $w_7^{(3-)}$ fragment with a m/Δm of >70,000 (FWHM). The high resolving power and dynamic range of the FTICR allows the monoisotopic masses and charge states for the overlapping distributions shown in inset (**b**) to be identified even though they differ by only 0.08 *m/z* units and have a signal intensity of <1% of the base peak.

oligonucleotides are illustrated in Figure 3 in which the IRMPD spectrum of a 4-10-4 MOE gapmer (***oligo2***) with the sequence 5′-GATGCCAGAGAGGATGCC-3′ is shown. Fragment types are indicated by different color bars with the bars representing the abundance of the 5′ fragment ions (a, a-B, b, and c) at the top of the figure and the 3′ fragments (w, x, and y) at the bottom. The fragment abundances were derived by integrating over all the

Table 1. Fragmentation coverage for the direct infusion of **oligo1**

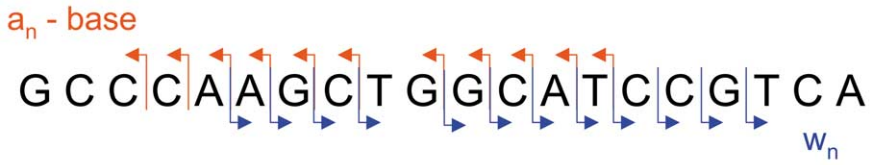

Fragment	Charge State	Fragment	Charge State
a3-base	1	w3	1
a4-base	1	w4	1,2
a5-base	1,2	w5	2
a6-base	2	w6	3
a7-base	2,3	w7	2,3
a8-base	2,3	w8	2,3,4
a9-base		w9	3,4
a10-base	3,4	w10	3,4
a11-base	3,4	w11	
a12-base	3,4,5	w12	5,6
a13-base	3,4,5,6	w13	4,5,6
a14-base	5	w14	4,6
		w15	5

charge states observed for each fragment ion. The oligonucleotide has a uniform phosphorothioate backbone with 2′ methoxyethyl modifications indicated by the underlined bases. In the MOE "wings", only low abundance b_n, c_n, x_n, and y_n fragment ions are observed while abundant a-base and w ions are observed in the 2′ deoxy "gap". It should also be pointed out that very few internal fragment ions are observed. For almost all of the cleavage sites, at least two charge states of the corresponding fragment ion and two types of fragment ions are observed. For example, both the $w_4^{(1-)}$ and $w_4^{(2-)}$ fragment ions as well as the $y_4^{(1-)}$, $y_4^{(2-)}$, and $y_4^{(3-)}$ fragment ions are observed corresponding to cleavage at four bases in front of the 3′ end of the gapmer. This redundant information provides assurance that the sequence is correctly assigned. For this gapmer, the redundant information is necessary since the b_6 and y_6 fragment ions have the identical mass. If the a_6-B and the w_6 ions were not identified, there would be ambiguity in the assigned sequence. Without the identification of the b_n, c_n, x_n, and y_n fragment ions necessary to sequence the MOE wings, the MOE gapmer could not be sequenced in its entirety. It is also worth pointing out that the complete sequence coverage is obtained InHex while less than 60% sequence coverage is achieved when standard in cell IRMPD protocols are employed as the in-cell approach typically generates fragments corresponding to only 5 or 6 bases from each end.

One obvious drawback of the InHex IRMPD scheme is that, because dissociation takes place in the hexapole ion reservoir (that operates in a non mass-selective manner), selective dissociation of low level impurities or specific components from mixtures is not possible. We expect this potential shortcoming to be resolved with the implementation of a mass selective quadrupole in front of the external ion reservoir; such an approach would allow *m/z* selection prior to accumulation and broadband dissociation [15–17]. We are presently implementing this modification and will describe the performance in a later publication. In lieu of a front-end mass filter to accommodate complex mixtures, one relatively straightforward solution is to perform an on-line separation and characterize each component by InHex IRMPD as it elutes. As described below, the not-so-obvious aspect of this approach is how to accomplish alternating MS and InHex MS/MS measurements without sacrificing the ionization duty cycle of the system during an on-line separation.

Application of InHex IRMPD with On-Line Separations—Dodging the Laser Beam

In a recent publication we demonstrated that when "sidekick" trapping is employed in the FTICR trapped ion cell, a large magnetron radius can result that renders on-axis IRMPD ineffective because the trajectory of the ion ensemble no longer intersects the central axis of the trapped ion cell [18]. We showed that this phenomenon could be exploited to effect *m/z* selective IRMPD dissociation by applying rf-tickle pulses that excited, either in an *m/z*-selective or a broadband mode, the cyclotron frequency of the orbiting ions such that their flight path intercepted the on-axis laser beam resulting in effective IRMPD [18]. Because we no longer use sidekick trapping and instead use only "gated trapping", this technique is no longer applicable to our work. However, an important lesson learned from that work, which is still very applicable to the methods we presently employ, is that the trajectory of ions in the trapped ion cell can be manipulated to either eliminate or maximize the interaction of the ion ensemble with an on-axis laser beam. Because ions captured with gated trapping have near-zero magnetron radii, irradiation with an on-axis laser beam produces significant overlap with the ion ensemble and extensive fragmentation.

Interestingly, if ions are trapped by gated-trapping, then excited to larger cyclotron radii, an on-axis laser beam (even at full power) has *no* effect on the ions because their trajectories no longer take them through the center of the trapped ion cell where they can cross the impinging laser beam. This effect is illustrated in Figure 4. The ESI-FTICR spectrum of ***oligo1*** was acquired with a 10.6 μm CO_2 laser firing at 25 watts during the entire 1.15 s detection event; the laser was triggered immediately *following* the chirp excite that promoted the ion ensemble to a larger cyclotron radius. The spectrum is absent of any IRMPD induced fragments and is indistinguishable from a control spectrum acquired with no laser event (data not shown). Note also that the $(M\text{-}5H^+)^{5-}$ and $(M\text{-}4H^+)^{4-}$ species still contain noncovalently associated piperidine/imidizole adducts, consistent with a very gentle ESI interface and inconsistent with in-cell activation [19]. The same molecular ions were completely dissociated in the trapped ion cell with only a 25 ms irradiation at 5 watts when the laser trigger *preceded* the rf-excite (data not shown).

Importantly, when the laser is aligned to traverse the central axis of the instrument (as illustrated in Figure 1), a post-excitation high power irradiation event can generate fragments in the hexapole concurrent with detection of intact ions in the trapped ion cell. Thus, by alternating between a post-excite laser-on scan and a laser-off scan, alternating MS and InHex IRMPD-MS/MS scans can be acquired. This scheme is illustrated in Figure 5. While intact species are being detected in scan n, ions are being accumulated and concurrently irradiated in the external ion reservoir for subsequent detection in the next scan (n + 1). Similarly, while InHex IRMPD fragment ions are being detected in scan n + 1, the molecular ions to be detected in scan n + 2 are being accumulated in the external ion reservoir, and so on and so on. This alternating MS, MS/MS approach is ideally suited for coupling with on-line separations that present pure compounds to the mass spectrometer in a temporally separated fashion. Figure 6 illustrates the application of this approach to a mixture of 3 oligonucleotides (***oligo1***, ***oligo3***, and ***oligo4***) that were separated using on-line μ-LC. The inset in

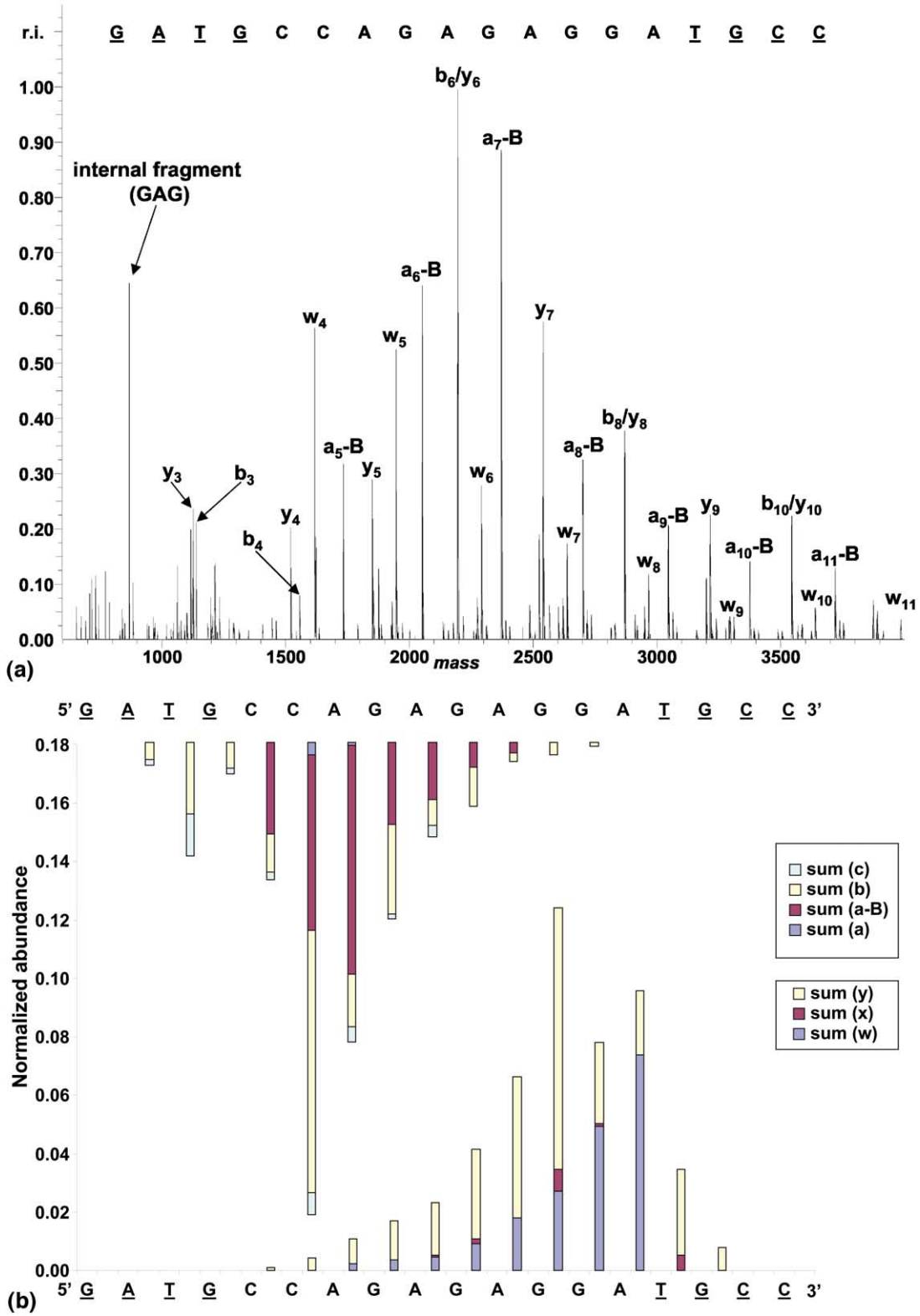

Figure 3. (**a**) Deconvoluted mass spectrum of the InHex IRMPD fragmentation of a gapmer oligonucleotide (***oligo2***). A continuous series of fragment ions corresponding to 11 bases in from both the 5′ and 3′ end are observed. The coverage map in (**b**) illustrates the extent (and type) of sequence coverage as a function of position and 2′ substituent.

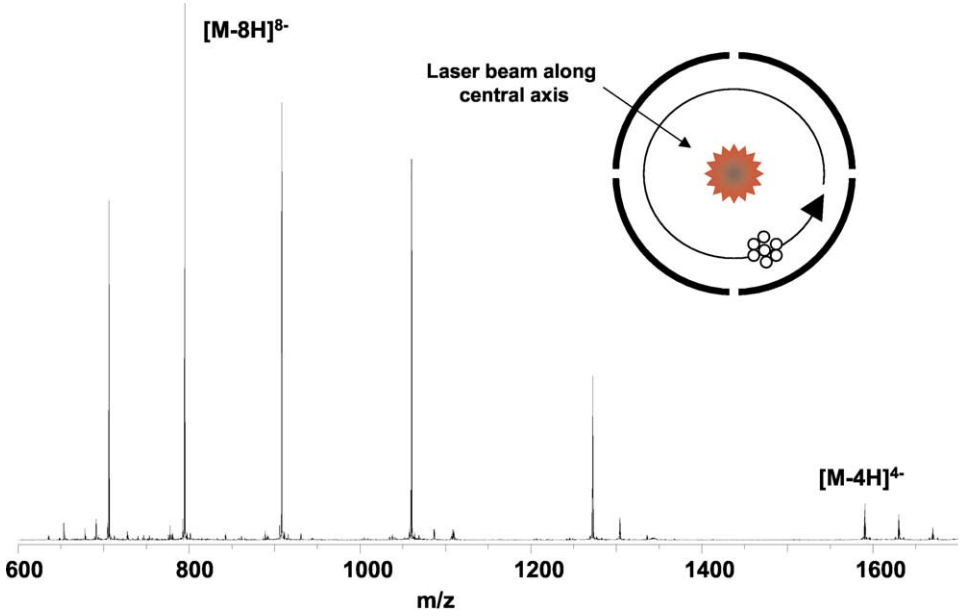

Figure 4. Laser "dodging" in the FTICR trapped ion cell: ESI-FTICR spectrum of ***oligo1***. Following ion injection and excitation of the ion ensemble to a larger cyclotron radius, a 25 watt 1.15 s laser pulse was sent through the center of the trapped ion cell. The resulting spectral response was unaffected by the laser pulse as the large cyclotron radius of the ion ensemble does not permit the ion trajectories to cross the laser beam.

Figure 6a illustrates the UV chromatogram demonstrating that the oligonucleotides are well separated chromatographically. The alternating MS InHex-IRMPD scheme described above (and illustrated schematically in Figure 5) was applied to the eluent of the LC column. The chromatographic conditions employed, while providing a reasonably high-quality separation, produced a relatively narrow distribution of low charge states in the mass spectra for the intact species owing to the 2 mM tripentylammonium acetate. The spectrum in Figure 6b illustrates the MS spectrum (acquired according to the scheme in Figure 5a) of intact ***oligo1***. The spectrum is dominated by the $(M - 4H^+)^{4-}$ species and is absent of any oligonucleotide fragment ions. The subsequently acquired spectrum of ***oligo1*** shown in Figure 6c illustrates the InHex IRMPD spectrum acquired according to the scheme in Figure 5b. This spectrum is dominated by fragment ions corresponding to a-base and w fragment ions. A key attribute of this approach is that the high ionization duty cycle of the ESI-FTICR detection scheme is maintained, as is the ability to perform InHex IRMPD of oligonucleotides on a time scale compatible with chromatographic separation. We intend to apply this approach to characterize low abundance synthetic oligonucleotide impurities and to interrogate metabolites of antisense compounds. Application of this approach in conjunction with the addition of a mass selective injection strategy should offer a significant increase in the working dynamic range of ESI-IRMPD-FTICR analyses.

Hollow Fiber Waveguide as a Conduit for IR Photons

One of the drawbacks of the on-axis InHex IRMPD scheme described above (and illustrated in Figure 1 is that obtaining "perfect" alignment of the laser beam from one end of the magnet to the external ion reservoir can be challenging. Additionally, because the vacuum chamber is on wheels and is occasionally rolled out of the magnet bore for maintenance or an extended bake out, re-alignment is not guaranteed upon re-insertion of the vacuum chamber. Furthermore, the on-axis approach may preclude the use of an on-axis electron filament for electron impact ionization or electron capture dissociation [20].

While bringing an IR laser beam directly into the hexapole ion reservoir orthogonal to the central axis should be possible with conventional optical components and IR-compatible windows, this approach would command a larger instrument footprint and would still suffer from potential alignment difficulties associated with moving the vacuum chamber. A fiber optic-based approach would be very attractive from the analytical instrumentation perspective as it would be robust, straightforward to align, and could be mounted on the vacuum chamber to move with the entire vacuum cart. Unfortunately, IR-compatible fiber optics capable of transmitting power in the range typically used for IRMPD are not available owing to the mutually exclusive properties the fiber material must possess: Flexibility and IR transmissivity. Recently, however, HFWG were developed to transmit very high power

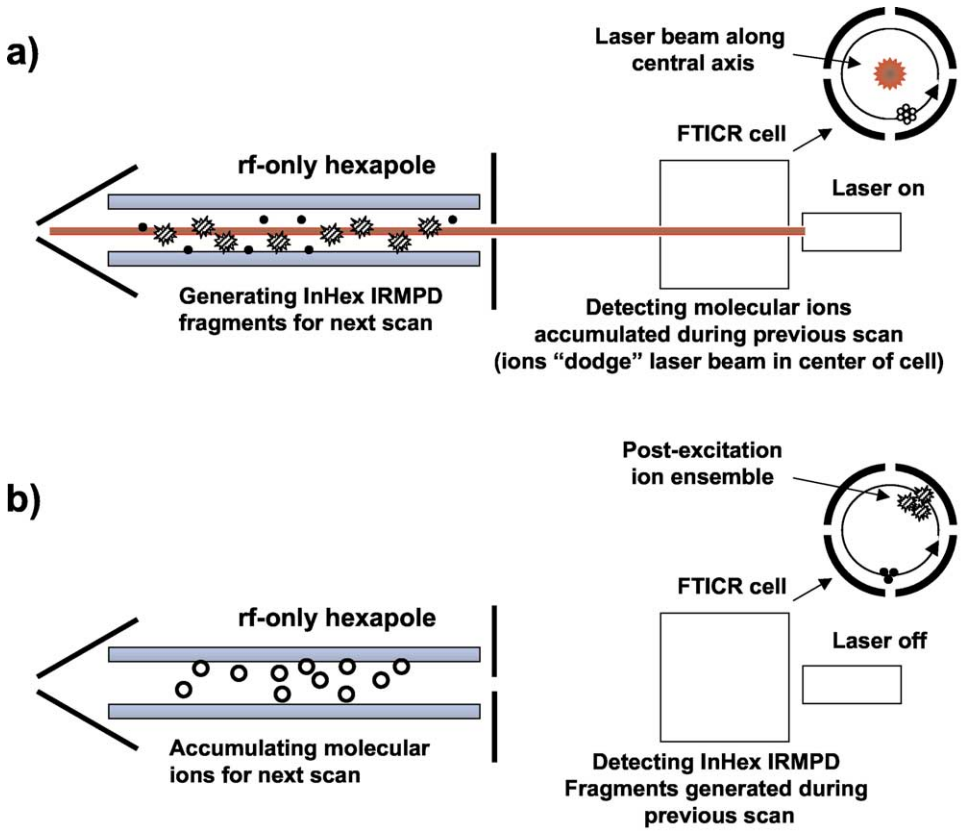

Figure 5. Scheme for alternating between MS and InHex IRMPD measurements. In the configuration depicted in (**a**) the laser beam is fired after the intact ions (accumulated on the previous scan) are excited to an expanded cyclotron radius. During the 1.15 s detection event, the laser is fired through the trapped ion cell and ion optics such that it impinges on the hexapole and generates InHex IRMPD fragments in the external ion reservoir. In the subsequent scan, the configuration depicted in (**b**) is employed in which the laser is turned off allowing intact ions to accumulate in the external ion reservoir while the InHex IRMPD fragments generated in the previous scan are analyzed in the trapped ion cell. Alternating between configuration (**a**) and (**b**) allows the alternating collection of MS and InHex IRMPD MS/MS spectra on a chromatographic time scale without a loss in ionization duty cycle. Molecular ions are depicted as open circles while fragment ions are depicted as shaded or filled shapes.

infrared radiation with high efficiency (e.g., losses as low as 0.1 dB/m and power transmission of 2.5 kW at 10.6 μm). Until our recent work [10], all HFWG applications published to date took place at or above atmospheric pressure while mass spectrometers operate at 6–12 orders of magnitude below atmospheric pressure. In order to make use of the high transmission efficiency and flexibility of the HFWG for MS applications, it must be adapted to serve as both an IR transmission medium and a vacuum feedthrough. In order to adapt the HFWG to work at reduced pressure and to bring IR photons directly into the external ion reservoir, a sealed vacuum interface was constructed as shown in Figure 7. As described in detail elsewhere [10], the waveguide assembly is attached directly to the faceplate of the IR laser via a set of small optical rails that provide both rigidity and crude alignment. The 3.5 mm diameter laser beam is focused through an aluminum aperture and into the HFWG assembly that enables operation at reduced pressure [10].

Initial experiments were performed with the 1 mm i.d. waveguide (o.d. = 1.6 mm) coupled to the external ion reservoir of the ESI-FTICR instrument. A 1 mm i.d. HFWG was brought into the region of the vacuum chamber containing the external ion reservoir such that it was orthogonal to the axis of the ion optics (Figure 7) resulting in the beam making a single pass across the longitudinal axis of the ion volume. HFWG-IRMPD studies with multiply charged oligonucleotide anions resulted in extensive fragmentation, comparable to that observed with the on-axis configuration, except that ~5-fold lower irradiation power could be utilized. The efficacy of this approach as applied to a 20-mer phosphorothioate oligonucleotide is illustrated in Figure 8. The ESI-FTICR spectrum of ***oligo1*** shown in Figure 8a was acquired following a 1 s external accumulation event in the absence of any laser irradiation. The spectrum is dominated by the charge state distribution of the intact oligonucleotide. The spectrum in Figure 8b was acquired under the same conditions as in Figure 8a except following the 1 s external ion accumulation event an, on-axis 50 ms, 10 watt laser pulse was applied.

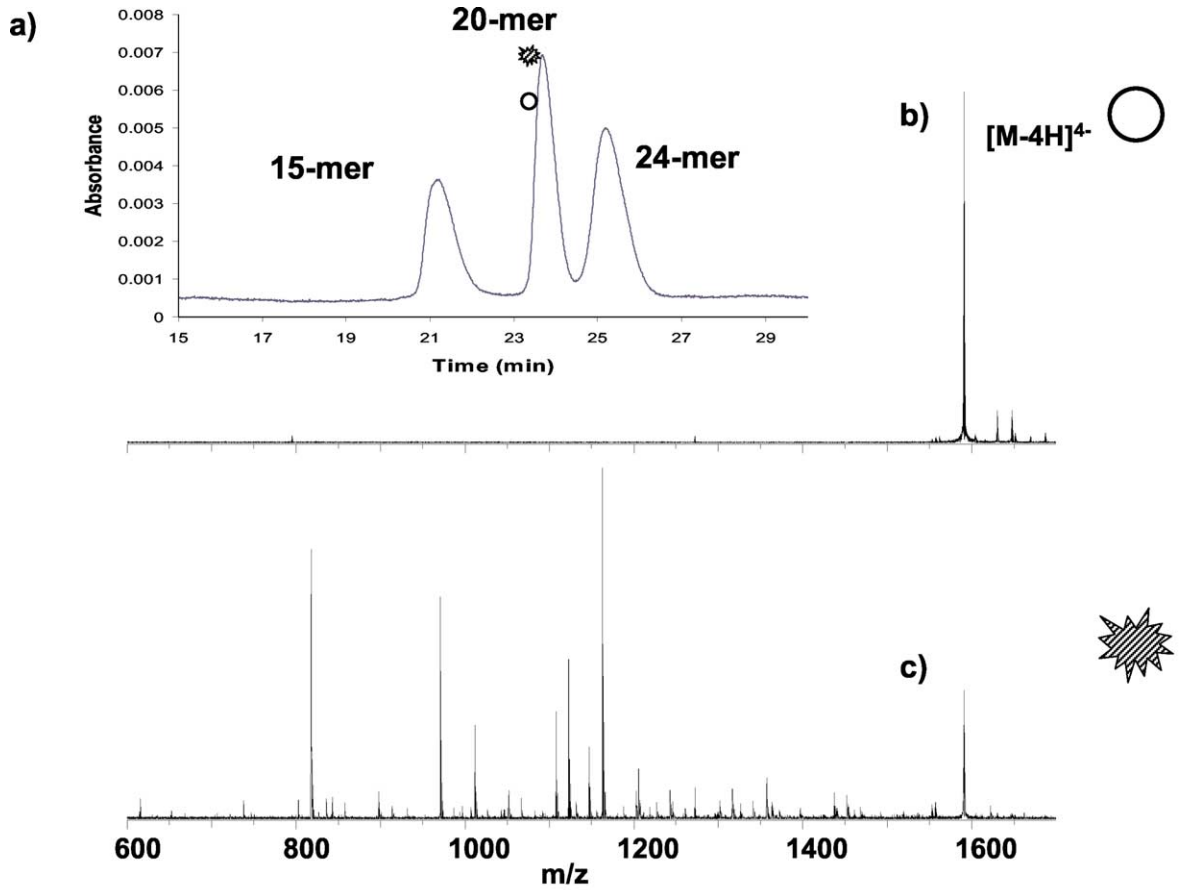

Figure 6. Application of the alternating pulse sequence illustrated in Figure 5. A mixture of three oligonucleotides is separated by on-line μ-HPLC and subjected to alternating MS and InHex IRMPD MS/MS analysis. The UV chromatogram in (**a**) illustrates that the three components are well separated chromatographically. The spectrum of ***oligo1*** shown in (**b**) was acquired using the scheme illustrated in Figure 5**a**) while the spectrum in (**c**) was acquired using the scheme in Figure 5**b**). See text.

Under these conditions the intact species still dominate the spectrum but the abundance of the higher charge states are attenuated and a few IRMPD fragments are evident such as the a_5–base, a_6–base, and w_3–A–H_2O species. The spectrum in Figure 8c was acquired under conditions identical to those em-

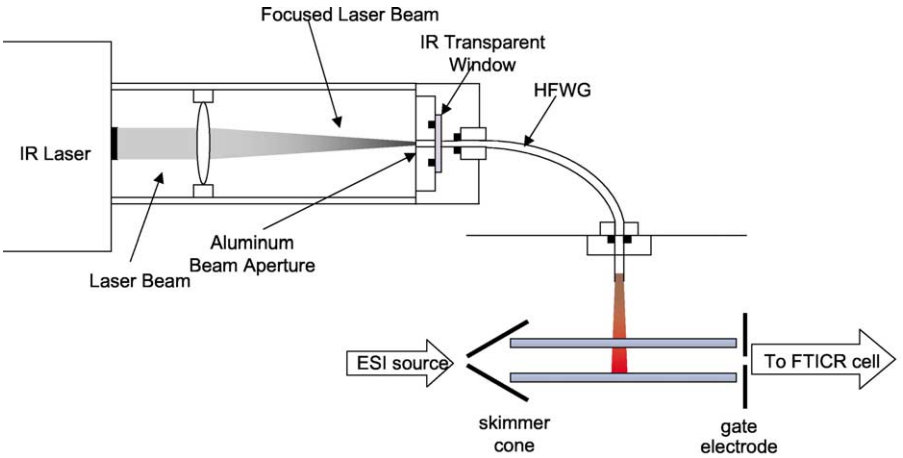

Figure 7. Schematic representation of the HFWG-IRMPD coupling approach used in this work. A single focusing lens and x,y manipulator are mounted on a set of small optical rails that mount directly to the faceplate of the CO_2 laser. The 1 mm waveguide as interfaced to the external ion reservoir of the ESI-FTICR instrument such that the beam exiting the HFWG intersects the ion reservoir orthogonal to the central axis.

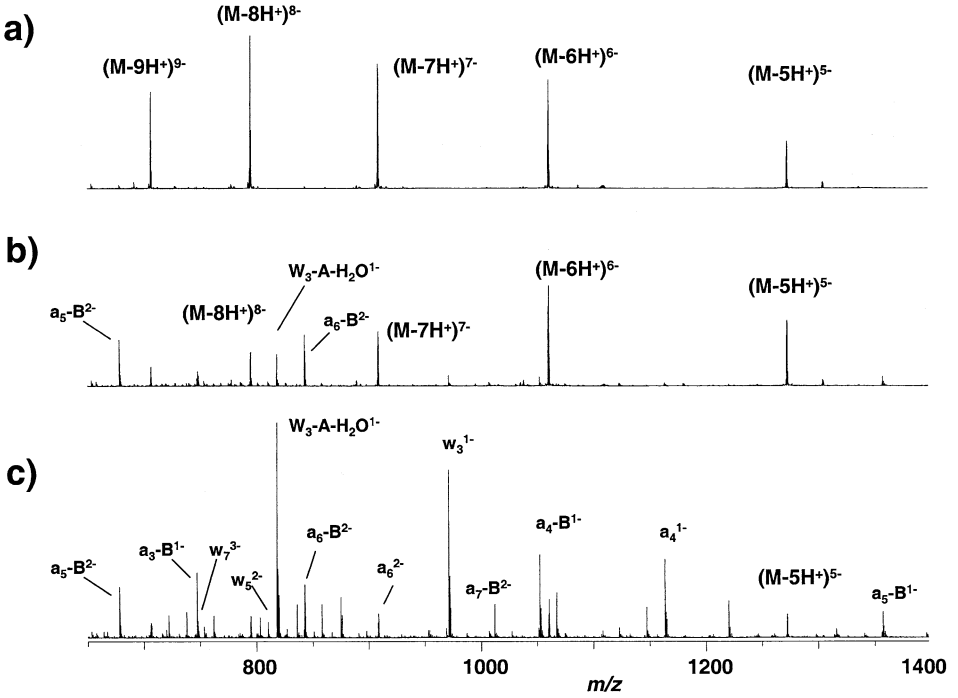

Figure 8. A comparison of InHex IRMPD of ***oligo1*** performed with the on-axis configuration depicted in Figure 1 and the HFWG configuration depicted in Figure 7. The spectrum in (**a**) was acquired without any laser irradiation and contains primarily intact molecular ions. The spectra in (**b**) and (**c**) were acquired following a 10 watt, 50 ms laser pulse employing the on-axis and HFWG configurations, respectively. In general the same types and abundances of fragments are observed with the on-axis and HFWG approaches except the power required by the HFWG approach is ~5× lower than that of the on-axis approach.

ployed in Figure 8b except the 50 ms, 10 watt laser pulse was applied through a 1 mm hollow fiber waveguide using the interface depicted in Figure 7. In this spectrum the majority of the molecular ions have undergone dissociation and the spectrum is dominated by a–base and w fragment ions. Interestingly, similar fragment abundances were obtained with the on-axis configuration when either 5× longer irradiation times or 5× higher irradiation powers were employed (data not shown). This difference is likely due to two primary factors. First, there is undoubtedly some beam attenuation due to the relatively long path length inherent in the on-axis configuration and the 4 mR beam divergence of the 3.5 mm beam. Perhaps more importantly, while the power density of the beam in the on-axis mode is less than the nascent laser beam, the power density of the laser exiting the HFWG is higher that the nascent laser beam. For example, the initial power density of the 10 watt 3.5 mm beam is about 1 watt/mm^2 while the power density out of the 1 mm wave guide for the same 10 watt beam (focused into the HFWG) is about 12.7 W/mm^2. As described in detail elsewhere, this HFWG approach is also applicable to interfacing an IR laser with a quadrupole ion trap; in those studies a 500 mm i.d. HFWG was employed resulting in nearly a 50-fold increase in power density relative to the nascent 3.5 mm beam [10]. Current studies are aimed at understanding the competing effects of collision cooling and IR vibrational activation in an attempt to optimize the dissociation efficiency while maintaining the favorable aspects of operating 2-D and 3-D traps at elevated high pressure.

Conclusions

In this work we explored several variations on InHex IRMPD for the characterization of modified oligonucleotides using an ESI-FTICR spectrometer. InHex IRMPD provides a comprehensive series of fragments allowing thorough characterization of a wide range of oligonucleotides containing alternative backbones and 2′ substitutions. The performance attributes of this approach were demonstrated with several modified oligonucleotides including an 18 nucleotide MOE gapmer. An alternative pulse sequence was presented that allows alternating MS and IRMPD MS/MS spectra to be acquired on a chromatographic timescale without loss in ionization duty cycle. Ions are excited to a larger cyclotron radius such that they "dodge" the IR laser beam that travels through the center of the trapped ion cell and impinges on the external ion reservoir creating IRMPD fragments that will be detected in the next scan. The utility of this

approach was generated with the on-line analysis of a mixture of 3 oligonucleotides. An alternative approach for directing IR radiation into the external ion reservoir using a 1 mm hollow fiber waveguide with a vacuum compatible mounting assembly was presented. This approach offers a simple and robust alternative to the previously utilized on-axis scheme and performs comparably to the on-axis approach except it requires ~5× lower laser power or ~5× shorter laser irradiation intervals.

References

1. Bomse, D. S.; Berman, D. W.; Beauchamp, J. L. Energetics of the Rearrangement of Neutral and Ionized Perfluorocyclopropane to Perfluoropropylene. Use of Infrared Multiphoton Dissociation Spectra to Identify Structural Isomers of Molecular Ions. *J. Am. Chem. Soc.* **1981,** *103,* 3967–3971.
2. Baykut, G.; Watson, C. H.; Weller, R. R.; Eyler, J. R. Infrared Multiple Dissociation of Some Oxygen-Containing Hydrocarbon Ions. Differentiation of Isomeric Ion Structures in the Gas Phase. *J. Am. Chem. Soc.* **1985,** *107,* 8036–8039.
3. Little, D. P.; Speir, J. P.; Senko, M. W.; O'Connor, P. B.; McLafferty, F. W. Infrared Multiphoton Dissociation of Large Multiply Charged Ions for Biomolecule Sequencing. *Anal. Chem.* **1994,** *66,* 2809–2815.
4. Little, D. P.; Aaserud, D. J.; Valaskovic, G. A.; McLafferty, F. W. Sequence Information from 42-108-mer DNAs (Complete for a 50-mer) by Tandem Mass Spectrometry. *J. Am. Chem. Soc.* **1996,** *118,* 9352–9359.
5. Tonner, D. S.; McMahon, T. B. Consecutive Infrared Multiphoton Dissociations in a Fourier Transform Ion Cyclotron Resonance Mass Spectrometer. *Anal. Chem.* **1997,** *69,* 4735–4740.
6. Hofstadler, S. A.; Sannes-Lowery, K. A.; Griffey, R. H. Infrared Multiphoton Dissociation in an External Ion Reservoir. *Anal. Chem.* **1999,** *71,* 2067–2070.
7. Li, W.; Hendrickson, C. L.; Emmett, M. R.; Marshall, A. G. Identification of Intact Proteins in Mixtures by Alternated Capillary Liquid Chromatography Electrospray Ionization and LC ESI Infrared Multiphoton Dissociation Fourier Transform Ion Cyclotron Resonance Mass Spectrometry. *Anal. Chem.* **1999,** *71,* 4397–4402.
8. Senko, M. W.; Hendrickson, C. L.; Emmett, M. R.; Shi, S. D. H.; Marshall, A. G. External Accumulation of Ions For Enhanced Electrospray Ionization Fourier Transform Ion Cyclotron Resonance Mass Spectrometry. *J. Am. Soc. Mass Spectrom.* **1997,** *8,* 970–976.
9. Hofstadler, S. A.; Sannes-Lowery, K. A.; Griffey, R. H. Infrared Multiphoton Dissociation in an External Ion Reservoir. *Anal. Chem.* **1999,** *71,* 2067−2070.
10. Drader, J. J.; Hannis, J. C.; Hofstadler, S. A. Infrared Multiphoton Dissociation with a Hollow Fiber Waveguide. *Anal. Chem.* **2003,** *75,* 3337−3412.
11. Crooke, S. T. Antisense Technology: Principles, Strategies and Applications. Crooke, S. T., Ed.; Marcel Dekker, Inc.: New York, 2001; pp 1–28.
12. Cook, P. D. *Antisense Research and Applications;* Crooke, S. T.; Lebleu, B., Eds.; CRC Press: Boca Raton, 1993; pp 149–187.
13. Sannes-Lowery, K. A., Hofstadler, S. A. Sequence Confirmation of Modified Oligonucleotides Using IRMPD in the External Ion Reservoir of an Electrospray Ionization Fourier Transform Ion Cyclotron Mass Spectrometer. *J. Am. Soc. Mass Spectrom.*, in press.
14. McLuckey, S. A.; Van Berkel, G. J.; Glish, G. L. Tandem Mass Spectrometry of Small, Multiply Charged Oligonucleotides. *J. Am. Soc. Mass Spectrom.* **1992,** *3,* 60–70.
15. Belov, M. E.; Nikolaev, E. N.; Anderson, G. A.; Auberry, K. J.; Harkewicz, R.; Smith, R. D. Electrospray Ionization-Fourier Transform Ion Cyclotron Mass Spectrometry Using Ion Preselection and External Accumulation for Ultrahigh Sensitivity. *J. Am. Soc. Mass Spectrom.* **2001,** *12,* 38−48.
16. Harkewicz, R.; Belov, M. E.; Anderson, G. A.; Pasa-Tolic, L.; Masselon, C. D.; Prior, D. C.; Udseth, H. R.; Smith, R. D. ESI-FTICR Mass Spectrometry Employing Data-Dependent External Ion Selection and Accumulation. *J. Am. Soc. Mass Spectrom.* **2002,** *13,* 144−154.
17. Marshall, A. G.; Chalmers, M. J.; Cooper, H. J.; Emmett, M. R.; Hakansson, K.; Hendrickson, C. L.; McFarland, M. A.; Quinn, J. P. *Abstract of Papers, 225th ACS National Meeting*, New Orleans, LA, March, 2003.
18. Hofstadler, S. A.; Sannes-Lowery, K. A.; Griffey, R. H. *m/z*-Selective Infrared Multiphoton Dissociation in a Penning Trap Using Sidekick Trapping and an rf-Tickle Pulse. *Rapid Commun. Mass Spectrom.* **2001,** *15,* 1−7.
19. Little, D. P.; McLafferty, F. W. Infrared Photodissociation of Noncovalent Adducts of Electrosprayed Nucleotide Ions. *J. Am. Soc. Mass Spectrom.* **1996,** *7,* 209−210.
20. McLafferty, F. W.; Horn, D. M.; Breuker, K.; Ge, Y.; Lewis, M. A.; Cerda, B.; Zubarev, R. A.; Carpenter, B. K. Electron Capture Dissociation of Gaseous Multiply Charged Ions by Fourier-Transform Ion Cyclotron Resonance. *J. Am. Soc. Mass Spectrom.* **2001,** *12,* 245−249.